Model-based parameter analysis of dielectric elastomer loudspeakers*

Giacomo Moretti[1] and Gianluca Rizzello[1]

***Abstract*— Dielectric elastomers (DEs) are polymeric multi-functional materials that can be used to develop lightweight electrostatic actuators. Among other, DEs allow developing coil-free loudspeakers, in which the acoustic diaphragm and the actuator are embedded into a single DE membrane, whose deformations are driven by electrostatic stresses.**
In this paper, we present a simulation analysis of a DE loudspeaker with the aim of highlighting the effect of relevant design parameters (namely, the DE membrane thickness, diameter, and geometric aspect ratio) on the acoustic response. For the sake of illustration, we make reference to a simple loudspeaker layout, which does not require any mechanical or pneumatic biasing elements, and only consists in a DE membrane pre-loaded off-plane. Based on a validated finite element multi-physics model of the system, we discuss how the system response (namely, eigenfrequencies and generated sound pressure level) varies with the design parameters. The presented results point out thresholds and trends that are relevant for the choice of DE loudspeakers' design parameters.

I. INTRODUCTION

Dielectric elastomers (DEs) are stretchable polymeric dielectrics that can be used to build electrostatic transducers [1]. DE actuators, in particular, make use of electrostatic forces generated within the deformable dielectric by an externally applied potential difference to produce strains that can surpass 100% [2]. Thanks to their ability to produce actuation strains over broad frequency ranges (up to several kilohertz), DEs provide a promising candidate for the development of coil-free loudspeakers made of soft electrode-covered DE membranes, which generate sound by means of voltage-driven vibrations of the membrane surface [3]. Several prototype demonstrators of DE loudspeakers have been developed in the past, which feature different layouts, such as pneumatically-biased domes [4], [5], flat panels [6], or push-pull speakers [7]. Recently, systematic attempts to model the dynamics and the acoustic response of DE loudspeakers have been also presented [8], [9], [10], [11]. Among other, such works have investigated the high-frequency dynamics and modal behaviour of DE membrane speakers, and the effect of sound pressure loads (namely, the acoustic impedance [12]) on the dynamic response.
To date, no systematic analysis of the effect of the design parameters (membrane thickness, dimensions) on the response of a DE loudspeaker has been presented. Whereas scaling criteria for the response of DE actuators working at low frequency are well-known (e.g., proportionality of the blocking force with the DE membrane thickness and surface), understanding the influence of design parameters on the response of a DE speaker is more complicated, because complex sound-structure interactions are involved, which demand for fully-coupled multi-physical descriptions.
In this article, we present a sensitivity analysis of DE loudspeakers response, with the aim of providing guidelines for the choice of some relevant design parameters. The analysis is carried out using a fully-coupled finite element (FE) model for DE loudspeakers, presented and validated in [13]. The model combines an electro-elastic model of a DE (treated as a hyperelastic membrane with ideal dielectric response) and a model of the surrounding acoustic domain, coupled in a bi-directional way. For the sake of the parametric analysis presented here, reference is made to a simple archetypal DE loudspeaker layout, which consists of a pre-stretched annular membrane pre-loaded off-plane in between a couple of fixed frames. This system is able to exploit voltage-driven vibrations (associated with the excitation of the vibration modes of the membrane) to generate sound. Using the FE model, we investigate how the frequency response (in terms of the sound level and the relevant eigenfrequencies) changes as a function of the design parameters (namely, DE thickness, radial dimensions, and device aspect ratio). We highlight quantitative trends for the dependence of the frequency response on the design parameters, and explain them in terms of simple scaling laws, that allow isolating the relative weight of different contributions (e.g., the membrane inertia vs. the acoustic impedance). The numerical data and the scaling laws reported in this paper can be used as a reference to guide the choice of design parameters for DE loudspeakers.

II. SYSTEM LAYOUT

We make reference to the DE membrane layout shown in Fig. 1. The active core of the device consists in an initially-flat circular DE membrane covered by compliant electrodes. The membrane is first uniformly pre-stretched in plane (i.e., its outer perimeter is rigidly attached on a rigid frame with diameter d_o, by applying a pre-stretch factor λ_p in all radial directions), then a rigid disc frame (with diameter d_i) is applied on the membrane centre and provided with an off-plane displacement h along the axis with respect to the outer frame. Both the inner and the outer frame are held fixed during operation.
Electrically, the DE membrane behaves as a deformable variable capacitor. By applying a voltage difference on the electrodes, Coulomb forces among the charges generate compressive electrostatic stresses along the membrane thickness

*This project has received funding from the European Union's Horizon 2020 research and innovation programme under the Marie Skłodowska-Curie grant agreement No 893674 (DEtune).

[1]The authors are with the Department of Systems Engineering, Saarland University, 66113 Saarbrücken, Germany {giacomo.moretti, gianluca.rizzello}@imsl.uni-saarland.de

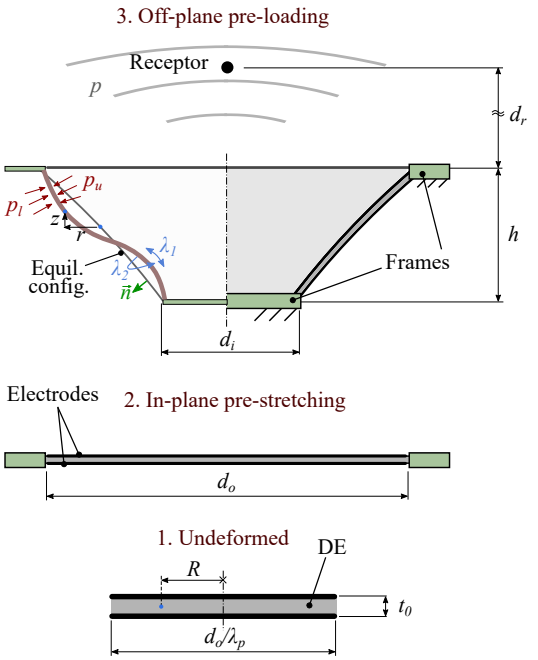

Fig. 1: Layout of the reference DE loudspeaker membrane. Bottom: undeformed mebrane ; Centre: flat pre-stretched membrane; Top: working configuration (cross-section).

(called Maxwell stresses), which result in a deformation of the DE. In most DE actuator layouts, Maxwell stresses are used to generate a linear stroke (or force). For the layout considered here, instead, applying a high-frequency voltage signal on the electrodes triggers structural vibrations of the membrane (perpendicular to the electrodes surface), which allow generating sound. As opposed to traditional dynamic cone loudspeakers, in which sound is generated by a pumping motion of a rigid diaphragm, here the sound is a result of the membrane's vibrations.

The device in Fig. 1 represents an archetypal version of a DE loudspeaker. Advanced loudspeaker designs might be developed based on this architecture by integrating the pre-loaded membrane in an enclosure or by developing a flexible array of multiple small-scale units [4]. Despite its simplicity, the system represents a suitable and simple benchmark for the parametric analyses discussed herein. The high-frequency dynamics and acoustic response of conically pre-loaded DE membranes have been investigated in our previous works [11], [13]. In particular, we observed that, upon high-frequency electrical excitation, conical DE membranes exhibit vibration mode shapes similar to those observed in flat annular tensioned membranes [14]. Furthermore, we showed that providing the system with an additional degree of freedom, by connecting the central disc frame to an elastic element and leaving it free to move axially, does not bring sensitive improvement in the acoustic response. This happens because the pass-band of such axial motion is limited to the low-frequency range, since the mass of the central disc frame is relatively large compared to the DE membrane's mass [10].

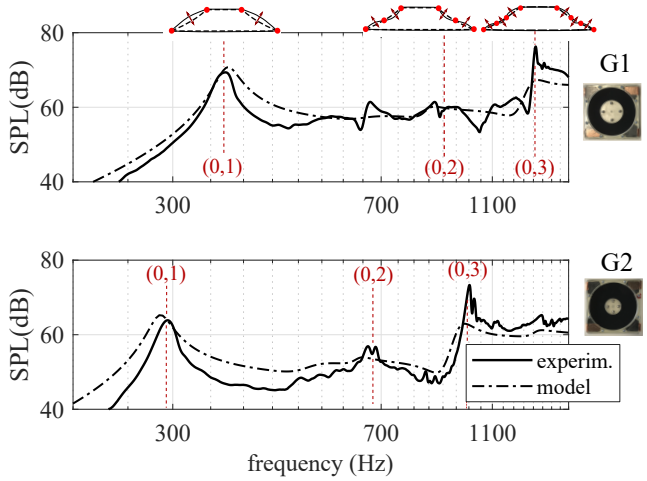

Fig. 2: FE model validation. The measured SPL of two different DE membrane layouts (G1 and G2) is plotted against FE model predictions.

III. MODEL AND VALIDATION

The dynamics of the DE membrane are governed by the following equations of motions (see [15]) for derivation):

$$\begin{cases} \rho R \dfrac{\partial^2 r}{\partial \tau^2} = \dfrac{\partial}{\partial R}\left(\dfrac{R\sigma_1}{\lambda_1^2}\dfrac{\partial r}{\partial R}\right) - \dfrac{R\lambda_2 p}{t_0}\dfrac{\partial z}{\partial R} - \dfrac{\sigma_2}{\lambda_2} \\ \rho R \dfrac{\partial^2 z}{\partial \tau^2} = \dfrac{\partial}{\partial R}\left(\dfrac{R\sigma_1}{\lambda_1^2}\dfrac{\partial z}{\partial R}\right) + \dfrac{R\lambda_2 p}{t_0}\dfrac{\partial r}{\partial R} \end{cases} \quad (1)$$

where R is the radial position of a generic material point on the undeformed membrane; τ is time; $r = r(R,\tau)$ and $z = z(R,\tau)$ are the radial and axial displacements of a point on the deformed membrane from the equilibrium configuration; ρ is the (constant) DE density; t_0 is the DE unstretched thickness; λ_1, λ_2 and σ_1, σ_2 are the local stretches and Cauchy stresses in the meridian and circumferential directions respectively; p expresses the contribution of the acoustic pressure (generated by the membrane motion), and it models the coupling between DE and air. The distribution of p in the surrounding of the DE is described by Helmholtz equation [12], [11]:

$$\begin{cases} \dfrac{\partial^2 p}{\partial \tau^2} = c_a^2 \nabla^2 p \\ \vec{n}\cdot\nabla p_l|_{S_f} = 0 \\ \vec{n}\cdot\nabla p_u|_{S_f} = 0 \\ \rho_a \vec{n}\cdot\nabla p_l|_{S_m} = -\vec{n}\cdot\dfrac{\partial^2 \vec{u}}{\partial \tau^2} \\ \rho_a \vec{n}\cdot\nabla p_u|_{S_m} = \vec{n}\cdot\dfrac{\partial^2 \vec{u}}{\partial \tau^2} \end{cases} \quad (2)$$

where $c_a = 343$ m/s is the sound speed in air; $\rho_a = 1.2$ kg/m^3 is the air density; ∇ and ∇^2 are the gradient and Laplace operators respectively; S_f and S_m indicate the surface of the frames and the membrane respectively; p_l and p_u are the evaluations of p on the upper or on the lower faces of the DE/frames respectively (as p assume different values on those different faces of such surfaces); $\vec{n}$ is the (two-dimensional) normal unit vector to the surface

TABLE I: Model parameters

DE material	Elastosil 2030 by Wacker
Extend. Mooney-Rivlin	$c_{1,0} = 194$ kPa
parameters	$c_{2,0} = 71$ kPa, $c_{0,1} = -24$ kPa
Mech. loss factor	$\eta_s = 0.15$
Permittivity	$\varepsilon = 2.8 \cdot 8.9 \cdot 10^{-12}$ F/m
DE density	$\rho = 1400$ kg/m^3

in the equilibrium pre-loaded configuration (pointing from the upper to the lower surface); and $\vec{u} = [r \ z]^T$ is the displacement vector for the membrane.

The DE is treated as a hyperelastic incompressible dielectric, i.e., the stresses depend on a strain-energy function Ψ, which in turn depends on the stretches and the applied electric field [16]. The following expressions hold:

$$\begin{aligned} &\hat{\sigma}_h = (1 + i\eta_s)\hat{\xi}_h, \ \xi_h = \lambda_h \frac{\partial \Psi}{\partial \lambda_h}, \text{ for } h = 1, 2, \text{ with} \\ &\Psi = \sum_{k=1} c_{k,0}(I_1 - 3)^k + \sum_{k=1} c_{0,k}(I_2 - 3)^k + \\ &- 0.5\varepsilon \left(\lambda_1 \lambda_2 E_L\right)^2, \\ &I_1 = \lambda_1^2 + \lambda_2^2 + (\lambda_1\lambda_2)^{-2}, \ I_2 = \lambda_1^{-2} + \lambda_2^{-2} + (\lambda_1\lambda_2)^2 \end{aligned} \tag{3}$$

where $\hat{x}$ denotes the frequency-domain representation of its corresponding time-domain signal x, $c_{k,0}$ and $c_{0,k}$ are coefficients of the extended Mooney-Rivlin hyperelastic model, ε is the DE permittivity, E_L is the nominal (Lagrangian) electric field, which is directly proportional to the applied voltage v, i.e., $E_L = v/t_0$, and is related to the actual electric field E on the material as follows:

$$E = \lambda_1 \lambda_2 E_L, \tag{4}$$

where factor $(\lambda_1\lambda_2)^{-1}$ represents the stretch along the thickness, owing to the material incompressibility. Material dissipation is modelled via a structural damping in the frequency domain, with loss factor η_d [8], [17].

Dynamics (1) and the acoustic pressure distribution p are solved for numerically using the FE model presented in [13]. The model is implemented in Comsol Multiphysics, and makes use of standard modules (Nonlinear Structural Material and Acoustics). The DE is modelled as a membrane component. The electro-mechanical coupling is implemented by modifying the default equation for the membrane strain energy function available in the software, so as to include the electrostatic contribution of E_L (Eq. (3)). The air domain surrounding the DE is modelled as a spherical volume holding a perfectly matched layer on its outer surface, which simulates an open infinite (or anechoic) domain. An arbitrary Lagrangian-Eulerian formulation (moving mesh) is used to consistently couple the membrane model (Lagrangian formulation) and the acoustic domain (Eulerian formulation). The model is able to calculate the eigenfrequencies and the frequency response of the system, subject to electrical excitation, by performing a linearisation of the DE response around the working configuration.

The model parameters are summarised in Tab. I, and they are the same as in [13]. A validation of the model against experimental tests is shown in Fig. 2, whereas an extensive multi-parameter validation is discussed in [13]. The picture shows the trend of the SPL as a function of frequency for two different DE membrane geometries. The samples are made of a silicone DE with initial thickness $t_0 = 100$ μm, outer diameter $d_o = 70$ mm and two different values of the aspect ratio ($\alpha = d_i/d_o$), namely: $\alpha = 0.50$ (G1) and $\alpha = 0.34$ (G2). The membranes have a pre-stretch $\lambda_p = 1.2$ and are mounted on a rigid baffle with outer diameter of 80 mm. For both membranes, the out-of-plane bias displacement is $h = 15$ mm. Measurements were performed in a sound-absorbing chamber, with a microphone located at a distance $d_r = 0.35$ m from the specimen along its axis. The membrane was excited with a voltage sweep with amplitude of 100 V, superimposed to a constant voltage bias of 3 kV (corresponding to an electric field in the range 50-60 kV/mm for the two configurations). For the aim of exemplification, the present analysis is restricted to a frequency range of up to 1500 Hz (although the device can generate sound over a larger frequency band), where the DE membranes' response features at least three recognisable vibration mode shapes (detectable via optical measurements, as discussed in [11]).

The DE membranes can steadily generate SPL over 50 dB for frequencies higher than first eigenfrequency (associated with the so-called mode $(0, 1)$), in correspondence of which the membrane deforms in a bubble-like fashion perpendicularly to its own surface. Three of the DE membranes eigenfrequencies/symmetrical deformation modes for the DE fall within the range shown in Fig. 2. Using the standard notation for membranes vibrations, we denote these modes $(0, n)$ (with n indicating the number of antinodes in the deformed shape). The acoustic response features a a clear peak in correspondence of the first mode, namely mode $(0, 1)$. Geometry G1 (with larger aspect ratio) is characterized by larger values of the frequencies of the eigenmodes (since h is the same for both membranes, G1, is subject to larger stretches and stresses in the meridian direction, parallel to the slant height) and produces larger values of SPL (see a discussion on this in Sect. IV-C). The model shows a good agreement with the measurements, as it is able to predict the relevant eigenfrequencies, the average trend of the SPL, and how the latter changes for different geometries.

IV. PARAMETRIC ANALYSIS RESULTS

We hereby use the FE model presented in [13] and validated in Fig. 2 to investigate the influence of some relevant design parameters on the acoustic performance of the DE membrane (e.g., working frequency range, SPL). Attention is set on the following parameters: 1) DE thickness; 2) membrane diameter; and 3) aspect ratio. In all the conducted studies, the material properties listed in Tab. I are used, and a constant distance $d_r = 0.35$ m (same as in Fig. 2) between microphone and sample is assumed. In all the presented analyses, attention is set on a restricted frequency range (up o 1500 Hz, as used in the validation presented in Fig. 2), which still allows highlighting the main trends of the frequency

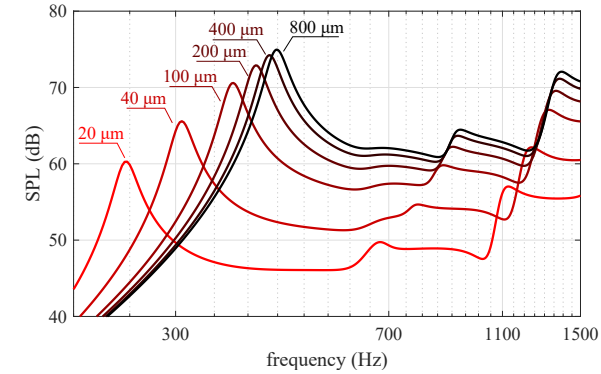

(a)

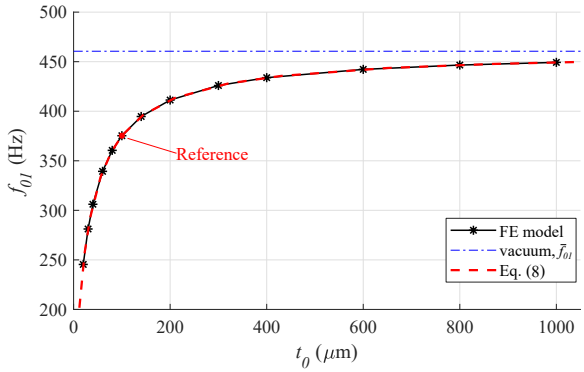

(b)

Fig. 3: (a) SPL as a function of the frequency for different values of t_0 (same proportions as G1 in Sect. III). (b) Eigenfrequency of mode $(0,1)$ as a function of t_0.

response (cut-in frequency of the sound generation range, modal response).

A. Membrane thickness

We consider a DE membrane loudspeaker with the same features, pre-load, and dimensions as G1 in Fig. 2, and we assume to vary the DE membrane thickness while keeping the nominal electric field E_L unaltered. Notice that, in practice, thickness scaling can be achieved either by varying the thickness of the dielectric layers, or by using multi-layer layouts, in which multiple membranes (each with a couple of electrodes) are stacked and connected in parallel. This latter solution allows increasing the thickness while limiting the voltage required to achieve a target electric field.

A comparison of the SPL frequency response obtained with different thickness is shown in Fig. 3a. The SPL level generated by the DE membrane increases with the thickness, until it reaches a saturation (visible, here, in the range 400-800 μm). As the acoustic pressure p enters dynamics (1) via a term proportional to t_0^{-1}, in the limit case of a very small DE thickness, the electrostatic loads on the dielectric are not able to overcome the pressure loads, hence resulting in a limited SPL. If the membrane thickness is very large, in contrast, pressure loads become negligible compared to the elastic, electrostatic and inertial loads acting on the membrane. In this latter case, the solution to (1) (and, hence, the resulting distribution of p and the associated SPL) becomes independent of the thickness.

Technically, p contributes in the membrane dynamics (in a lumped fashion) via frequency-dependent radiation damping and added mass contributions [12]. Because of the acoustic added mass, the eigenfrequencies of the system decrease by decreasing the thickness (see for example the peaks in SPL associated to mode $(0,1)$), as opposed to the eigenfrequencies of a membrane vibrating in vacuum, which only depend on the stress-to-density ratio and the radial dimensions (but not on the thickness) [12]. The eigenfrequency f_{01} of mode $(0,1)$ (i.e., the first relevant frequency for the acoustic response) calculated with the FE model at different values of t_0 are plotted in Fig. 3b (markers) and compared with the eigenfrequency $\bar{f}_{01}$ in vacuum (dash-dot line). As t_0 increases, f_{01} approaches $\bar{f}_{01}$ asymtpotically, since the contribution of the acoustic mass becomes negligible compared to the membrane inertia. If t_0 is small, in contrast, the acoustic added mass causes a sensible reduction in the DE natural frequency compared to $\bar{f}_{01}$. To further motivate this trend, we postulate that f_{01} can be expressed, in an approximate manner, as:

$$f_{01} = \frac{1}{2\pi}\sqrt{\frac{k_{01}^d}{m_{01}^d + m_{01}^a}} = \frac{1}{2\pi}\sqrt{\frac{k_{01}^d}{m_{01}^d\,(1+r_m)}} = \\ = \frac{\bar{f}_{01}}{\sqrt{1+r_m}}, \tag{5}$$

where k_{01} is a lumped modal stiffness [18] for the DE (associated to mode $(0,1)$), m_{01}^d is the modal mass due to the DE inertia, and m_{01}^a is the modal air mass contribution. The eigenfrequencies of membranes vibrating in vacuum scale proportionally to the inverse of the diameter and are independent of the membrane thickness [12]. We indicate with (d_o^{ref}, t_0^{ref}) a given combination of DE diameter and thickness (i.e., a reference configuration) and with $\bar{f}_{0,1}^{ref}$ the corresponding value of the eigenfrequency of mode $(0,1)$ in vacuum. The eigenfrequency $\bar{f}_{0,1}$ for a generic choice (d_o, t_0) of the parameters relates to $\bar{f}_{0,1}^{ref}$ as follows:

$$\bar{f}_{0,1} = \frac{d_o^{ref}}{d_o}\bar{f}_{0,1}^{ref} \tag{6}$$

Moreover, since m_{01}^d is expected to scale proportionally to $d_o^2 t_0$, whereas the acoustic mass m_{01}^a goes with d_o^3 (see, e.g., Eq. (7.5.15) in [12]), the ratio $r_m = m_{01}^a/m_{01}^d$ scales proportionally to $d_o t_0^{-1}$. Based on the argument above, by indicating with r_m^{ref} the value of r_m obtained in a reference configuration (as defined above), the value of r_m for a generic design can be expressed as follows:

$$r_m = \frac{d_o}{d_o^{ref}}\frac{t_0^{ref}}{t_0} r_m^{ref}, \text{ with } r_m^{ref} = \left(\frac{\bar{f}_{01}}{f_{01}^{ref}}\right)^2 - 1, \tag{7}$$

where f_{01}^{ref} represents the value of f_{01} in the reference configuration, and its dependency on $\bar{f}_{01}$ and f_{01}^{ref} has

been obtained using (5). Combining (5)-(7), the following relationship is obtained:

$$f_{01} = \frac{d_o^{ref}}{d_o} \frac{\bar{f}_{01}^{ref}}{\sqrt{1 + \frac{d_o}{d_o^{ref}} \frac{t_0^{ref}}{t_0} \left[\left(\frac{\bar{f}_{01}^{ref}}{f_{01}^{ref}} \right)^2 - 1 \right]}}, \quad (8)$$

We take $t_0^{ref} = 100$ μm and $d_o^{ref} = 70$ mm (same as in Fig. 2) as reference. Using the values of $\bar{f}_{01}$ and f_{01}^{ref} obtained from the FE model for the reference case, the trend of f_{01} as a function of t_0 based on (8) is represented in Fig. 3b with dashed line. Scaling law (8) consistently predicts the trend of f_{01} (with differences of less than 2% with respect to the actual values extracted from the FE model), hence confirming that the dependency of f_{01} on the thickness owes to relative values of the inertial and acoustic mass contributions.

The previous analysis suggests that the choice of the thickness for a DE membrane loudspeaker should represent a trade off between loss of performance (in terms of SPL) associated with very thin membranes, sensitive to the aeroacoustic loads, and a saturation in the achievable performance with an increase in the DE thickness.

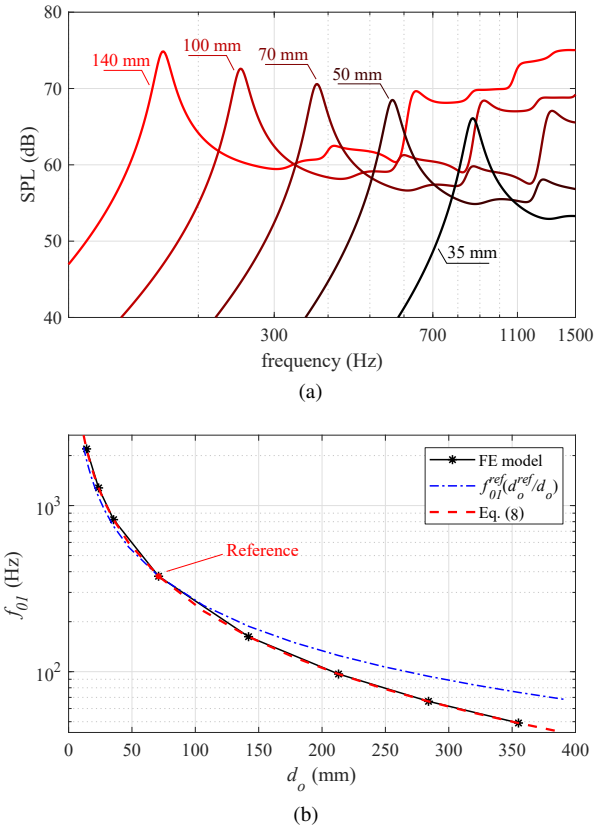

Fig. 4: (a) SPL as a function of the frequency for different values of d_o (same proportions as G1 in Sect. III). (b) Eigenfrequency of mode $(0,1)$ as a function of d_o.

B. Radial dimensions

Taking a DE membrane loudspeaker with the same features as G1 in Fig. 2 as reference, we hereby analyse the effect of scaling the membrane diameter d_o while keeping the thickness, the applied voltage and the proportions unchanged (i.e., d_i and h are scaled by the same factor as d_o). A comparison of the frequency-SPL trend for different values of d_o is shown in Fig. 4a. The distance between receptor point and DE is the same in all cases and equal to $d_r = 0.35$ m. Increasing the diameter causes the SPL to increase and the eigenfrequencies to decrease (see, e.g, the abscissas of the first peak). To evaluate such increase in relation to the radial scale factor, we recall that, for a monopole in free space, the radiated sound is proportional to the square of the frequency f, the amplitude of the displacement (e.g., either r or z in (1)), the area of the radiating surface, and the inverse of the distance from the receptor point (see, e.g., Eq. (9.5) in [19]), namely:

$$p \propto f^2 z d_o^2 d_r^{-1} \quad (9)$$

Although the radiated field from a complex surface features a complex distribution (which passes through the solution of (2) and cannot be expressed in terms of a close-form analytical expression), Eq. (9) still provides a structure that allows inferring proportionality relationships between p and the other variables. We also recall that, in a membrane vibrating in vacuum (i.e., not subject to air pressure loads), the eigenfrequencies are proportional to the inverse of the diameter, and the oscillation amplitude (displacement) in the presence of a fixed bulk excitation scales proportionally with the diameter [12]. This can be easily understood, e.g., by considering (1), neglecting the terms in p, and noticing that if the lateral dimensions (R), the displacements (r, z), and time τ are multiplied by a same scale factor, then the equations of motion remain unchanged. Based on that, assuming that the frequency f is actually proportional to d_o^{-1}, displacement r is proportional to d_o, and the distance source-receptor (d_r) is constant, p should scale proportionally with d_o, based on (9). The results of Fig. 4a, however, show that p scales in a sub-linear manner with d_o: increasing d_o by a factor 4 (from 35 mm to 140 mm), the value of the first SPL peak varies by 8 dB (i.e., a factor of 2.5 on the amplitude of p). This is, again, an effect of the aerodynamic loads, which (for a given membrane thickness) have greater effect on larger-diameter membranes, and prevent the achievable displacement amplitude to increase proportionally with the radius.

The trend of the eigenfrequency of mode $(0,1)$ vs. d_o is shown in Fig. 4b (markers). Considering a reference configuration (with diameter d_o^{ref}) and simply scaling the corresponding value f_{01}^{ref} of the eigenfrequency proportionally with the inverse of d_o (i.e., the same way as the eigenfrequencies would scale in vacuum - see Eq. (6)) leads to an underestimation at smaller scales and an even more significant overestimation of the eigenfrequency at larger scales (dash-dot line). Accounting for the effect of the aerodynamic loads and scaling the reference eigenfrequency

by using Eq. (8), however, provides a consistent estimate of the eigenfrequencies trend (dashed line), pointing out once again the relevance of the acoustic impedance on the DE dynamics.

C. Aspect ratio

We finally investigate the effect of the membrane aspect ratio, $\alpha = d_i/d_o$, on the acoustic response. We consider a set of DE membranes with the same outer diameter d_o, initial thickness t_0, and off-plane biasing displacement h as the membranes considered in Fig. 2. We then consider different values for the aspect ratio α. Assuming that the same voltage (i.e., the same nominal electric field E_L) is applied in all cases, the resulting SPL trends are given by the solid lines in Fig. 5a. Increasing α while keeping the ratio h/d_o constant results in an increase in the membrane meridian stretch λ_1^0 in the equilibrium configuration. For the cone DE layout considered here, the membrane average meridian stretch can be roughly estimated as follows (based on available lumped-parameter models of cone DE actuators [20]):

$$\lambda_1^0 \approx \lambda_p \frac{\sqrt{(d_o - d_i)^2 + 4h^2}}{d_o - d_i} = \\ = \lambda_p \frac{\sqrt{(1-\alpha)^2 + 4(h/d_o)^2}}{1-\alpha}, \tag{10}$$

and it increases monotonically with α, whereas the circumferential stretch at equilibirum λ_2^0 can be assumed independent of α and equal to the pre-stretch: $\lambda_2^0 = \lambda_p$. Because of the increase in λ_1^0 (and, hence, in stress), the frequency response of the membrane shifts towards right (e.g., the eigenfrequencies increase) by increasing α. Also the peak value of the SPL increases with α. A reason for that is the fact that, in the presence of larger stretches (i.e., when α is higher), the actual electric field E (as opposed to the nominal electric field E_L) applied on the membrane is larger (see Eq. (4)), resulting in larger-magnitude excitation. We repeat the calculation of the SPL for the different cases, scaling the nominal electric field E_L (bias + amplitude) proprotionally to the thickness, so as to obtain same actual electric field for all α:

$$E_L = E_L^{ref} \frac{\lambda_1^{0,ref}}{\lambda_1^0} \tag{11}$$

where E_L^{ref} and $\lambda_1^{0,ref}$ are the nominal field and equilibrium meridian stretch for a reference configuration (here, $\alpha = 0.5$, i.e., same as G1 in Fig. 2). The resulting trends of the SPL are shown in dashed line in Fig. 5a. The differences among the SPL peak values at different α is lower than in the case with invariant nominal field (solid lines). Larger values of α still result in larger peak values of the SPL, in spite of a decrease in the radiating surface and an increase in stiffness. This is ascribable to an increase in the excitation action owing to geometric effects. Smaller α causes the angle between the membrane profile and the horizontal plane to decrease, hindering the DE ability to vibrate off-plane (in the limit case of a horizontal membrane, no off-plane vibrations are virtually developed by the electric field [11]).

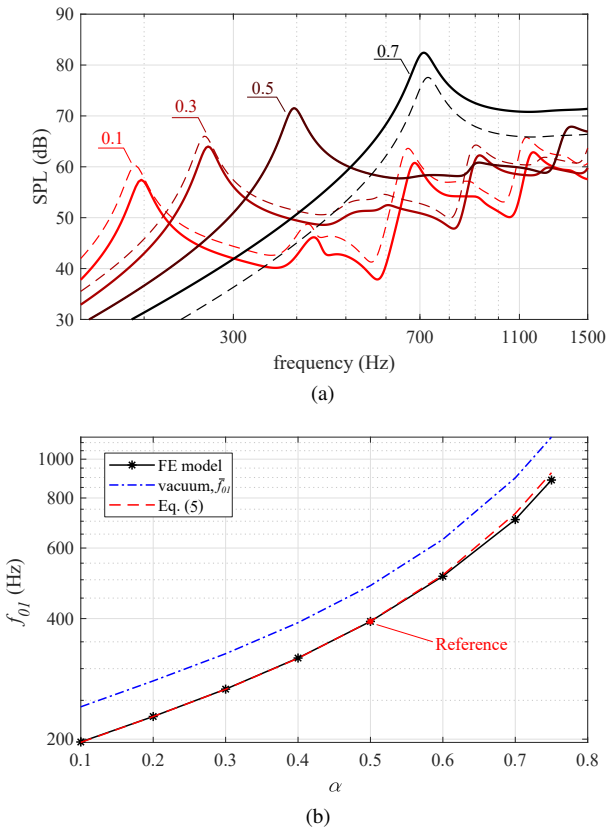

Fig. 5: (a) SPL as a function of the frequency for different values of α (same d_o and t_0 as G1 and G2 in Sect. III). Solid-line plots are obtained assuming same E_L for all cases, whereas dashed lines are obtained by keeping the actual electric field unchanged (b) Eigenfrequency of mode $(0,1)$ as a function of α.

The trend of the eigenfrequency of mode $(0,1)$ as a function of α predicted by the FE model is shown in Fig. 5b (markers), assuming same E_L for all cases. Increasing α makes f_{01} bigger as a consequence of an increase in stress. The trends of f_{01} is compared with that of $\bar{f}_{01}$ (i.e., the eigenfrequency in vacuum, calculated with the FE model), represented with dash-dot line in the plot. For all α, the two frequencies (f_{01}, $\bar{f}_{01}$) differ by a nearly-constant factor, owing to the acoustic mass. We extract a value of r_m for a reference case ($\alpha = 0.5$) from Eq. (5), using the eigenfrequencies calculated via the FE model. We then use the obtained value (namely, $r_m = 0.506$) to predict $f_{0,1}$ from the trend of $\bar{f}_{01}$ for all other values of α using Eq. (5) (dashed line in Fig. 5b). By doing so provides an accurate prediction of the actual trend of $f_{0,1}$, hence confirming that the mass ratio r_m is roughly independent of α for the DE layout under investigation. Among other, this information provides a practical mean to obtain accurate predictions of a conical DE membrane dynamic response and eigenfrequencies without the need to resort to complex fully-coupled elasto-acoustic models.

V. CONCLUSIONS

We have presented a parameter analysis of the performance of loudspeakers made of dielectric elastomers (DEs), with the aim of providing general indications for the selection of design parameters. For the sake of exemplification, we set the attention on a simple DE speaker layout, which consists in an annular electrode-covered membrane deformed out-of-plane (in a conical fashion) in between a couple of fixed frames, and vibrated by the electrostatic stresses. We introduced a finite element model of the system, which has been proposed and validated in the past. The model couples, in a bi-directional fashion, an electro-elastic model of the DE and a model of the surrounding acoustic domain. We then used the model to evaluate the effect of some relevant design parameters (membrane thickness, diameter, and aspect ratio) on the system response. Results of the numerical simulations provide the following indications and design guidelines:

- increasing the thickness of a DE membrane increases the sound pressure level (SPL) that the device can produce only within a certain range, where the DE is subject to large acoustic loads (higher or comparable to the elastic and inertial loads). Whereas using excessively thin membrane severely limits the DE's ability to generate sound, increasing the thickness over a certain threshold would result in a saturation in the achievable SPL. The choice of a trade-off thickness should thus keep into consideration the contribution of the acoustic pressure loads on the DE dynamics.
- Increasing the radial dimensions of the membrane has the double effect of increasing the achievable SPL and shifting the range where the DE membrane starts producing sound towards the low frequency region. Also in this case, the achievable increase in SPL that can be obtained by increasing the speaker radial dimensions (while keeping the DE thickness constants) is limited by the acoustic loads, whose relevance increases with the size. Specifically, the generated acoustic pressure increases less than proportionally with the surface area, unless the thickness is consistently increased so as to mitigate the effect of the acoustic impedance.
- In the case of a circular DE pre-loaded off-plane, changing the aspect ratio and the geometric proportions of the membrane has a significant impact on the performance, as it affects the electrical excitation perceived by the DE in the presence of a same electric field. An aspect ratio that provides a larger inclination angle of the membrane with respect to the horizontal provides a significant increase in SPL, as it increases the DE's ability to generate off-plane velocities in response to a given electric field.

Although the practical design of a DE loudspeaker would require consideration of other aspects (e.g., design of baffles/enclosures, presence of damping elements, etc.), this study points out that a systematic characterisation of the coupled electro-elasto-acoustic dynamics (by means of coupled-models, or a combination of experimental tests and scaling laws) is key to guide the choice of design parameters.

REFERENCES

[1] F. Carpi, D. De Rossi, R. Kornbluh, R. E. Pelrine, and P. Sommer-Larsen, *Dielectric elastomers as electromechanical transducers: Fundamentals, materials, devices, models and applications of an emerging electroactive polymer technology*. Elsevier, 2011.

[2] R. Pelrine, R. Kornbluh, Q. Pei, and J. Joseph, "High-speed electrically actuated elastomers with strain greater than 100%," *Science*, vol. 287, no. 5454, pp. 836–839, 2000.

[3] Z. Zhao, C. Shuai, Y. Gao, E. Rustighi, and Y. Xuan, "An application review of dielectric electroactive polymer actuators in acoustics and vibration control," in *Journal of Physics: Conference Series*, vol. 744, no. 1. IOP Publishing, 2016, p. 012162.

[4] R. Heydt, R. Pelrine, J. Joseph, J. Eckerle, and R. Kornbluh, "Acoustical performance of an electrostrictive polymer film loudspeaker," *The Journal of the Acoustical Society of America*, vol. 107, no. 2, pp. 833–839, 2000.

[5] N. Hosoya, S. Baba, and S. Maeda, "Hemispherical breathing mode speaker using a dielectric elastomer actuator," *The Journal of the Acoustical Society of America*, vol. 138, no. 4, pp. EL424–EL428, 2015.

[6] E. Rustighi, W. Kaal, S. Herold, and A. Kubbara, "Experimental characterisation of a flat dielectric elastomer loudspeaker," in *Actuators*, vol. 7, no. 2. Multidisciplinary Digital Publishing Institute, 2018, p. 28.

[7] T. Sugimoto, A. Ando, K. Ono, Y. Morita, K. Hosoda, D. Ishii, and K. Nakamura, "A lightweight push-pull acoustic transducer composed of a pair of dielectric elastomer films," *The Journal of the Acoustical Society of America*, vol. 134, no. 5, pp. EL432–EL437, 2013.

[8] E. Garnell, C. Rouby, and O. Doaré, "Dynamics and sound radiation of a dielectric elastomer membrane," *Journal of Sound and Vibration*, vol. 459, p. 114836, 2019.

[9] E. Garnell, O. Doaré, and C. Rouby, "Coupled vibro-acoustic modeling of a dielectric elastomer loudspeaker," *The Journal of the Acoustical Society of America*, vol. 147, no. 3, pp. 1812–1821, 2020.

[10] G. Moretti, G. Rizzello, M. Fontana, and S. Seelecke, "A multi-domain dynamical model for cone-shaped dielectric elastomer loudspeakers," in *Electroactive Polymer Actuators and Devices (EAPAD) XXIII*, vol. 11587. International Society for Optics and Photonics, 2021, p. 115871K.

[11] ——, "High-frequency voltage-driven vibrations in dielectric elastomer membranes," *Mechanical Systems and Signal Processing*, vol. 168, p. 108677, 2022.

[12] L. E. Kinsler, A. R. Frey, A. B. Coppens, and J. V. Sanders, *Fundamentals of acoustics*. John Wiley and Sons, 1999.

[13] G. Moretti, G. Rizzello, M. Fontana, and S. Seelecke, "Finite element modelling of the vibro-acoustic response in dielectric elastomer membranes," in *Electroactive Polymer Actuators and Devices (EAPAD) XXIIV*. International Society for Optics and Photonics, 2022.

[14] M. Jabareen and M. Eisenberger, "Free vibrations of non-homogeneous circular and annular membranes," *Journal of Sound and Vibration*, vol. 240, no. 3, pp. 409–429, 2001.

[15] R. Vertechy, G. P. P. Rosati, and M. Fontana, "Reduced model and application of inflating circular diaphragm dielectric elastomer generators for wave energy harvesting," *Journal of Vibration and Acoustics*, vol. 137, no. 1, pp. 011 016–1–011 016–9, 2015.

[16] E. Hajiesmaili and D. R. Clarke, "Dielectric elastomer actuators," *Journal of Applied Physics*, vol. 129, no. 15, p. 151102, 2021.

[17] W. W. Soroka, "Note on the relations between viscous and structural damping coefficients," *Journal of the Aeronautical Sciences*, vol. 16, no. 7, pp. 409–410, 1949.

[18] M. Aenlle, M. Juul, and R. Brincker, "Modal mass and length of mode shapes in structural dynamics," *Shock and Vibration*, vol. 2020, 2020.

[19] M. Kleiner, *Acoustics and audio technology*. Fort Lauderdale, FL: J. Ross Publishing, 2011.

[20] G. Berselli, R. Vertechy, G. Vassura, and V. Parenti-Castelli, "Optimal synthesis of conically shaped dielectric elastomer linear actuators: design methodology and experimental validation," *IEEE/ASME Transactions on Mechatronics*, vol. 16, no. 1, pp. 67–79, 2011.